

Electronic properties of molecular solids: the peculiar case of solid picene

This article has been downloaded from IOPscience. Please scroll down to see the full text article.

2010 New J. Phys. 12 103036

(<http://iopscience.iop.org/1367-2630/12/10/103036>)

View [the table of contents for this issue](#), or go to the [journal homepage](#) for more

Download details:

IP Address: 161.111.180.191

The article was downloaded on 18/04/2012 at 10:30

Please note that [terms and conditions apply](#).

Electronic properties of molecular solids: the peculiar case of solid picene

Friedrich Roth^{1,3}, Matteo Gatti², Pierluigi Cudazzo²,
Mandy Grobosch¹, Benjamin Mahns¹, Bernd Büchner¹,
Angel Rubio² and Martin Knupfer¹

¹ IFW Dresden, PO Box 270116, D-01171 Dresden, Germany

² Nano-Bio Spectroscopy Group and ETSF Scientific Development Centre,
Dpto. Física de Materiales, Universidad del País Vasco, Centro de Física
de Materiales CSIC-UPV/EHU-MPC and DIPC, Avenue Tolosa 72,
E-20018 San Sebastián, Spain

E-mail: f.roth@ifw-dresden.de

New Journal of Physics **12** (2010) 103036 (8pp)


Received 19 August 2010

Published 20 October 2010

Online at <http://www.njp.org/>

doi:10.1088/1367-2630/12/10/103036

Abstract. Recently, a new organic superconductor, K-intercalated picene, with high transition temperatures T_c (up to 18 K) has been discovered. We have investigated the electronic properties of an undoped relative of this superconductor, solid picene, using a combination of experimental and theoretical methods. Our results provide deep insights into the occupied and unoccupied electronic states.

 Online supplementary data available from stacks.iop.org/NJP/12/103036/mmedia

Contents

1. Introduction	2
2. Methods	2
3. Results and discussion	4
4. Summary	7
Acknowledgments	7
References	7

³ Author to whom any correspondence should be addressed.

1. Introduction

Molecular crystals—built of π conjugated molecules—have been the focus of attention of researchers for many reasons. Within this class of materials, almost every ground state can be realized at will, spanning from insulators to semiconductors, metals, superconductors or magnets. Due to their relatively open crystal structure, their electronic properties can be easily tuned by the addition of electron acceptors and donors. In some cases, this has resulted in intriguing and unexpected physical properties. A prominent example of the latter is the formation of metallic, superconducting or insulating phases in the alkali metal-doped fullerides depending on their stoichiometry [1]–[4]. In particular, the superconducting fullerides (e.g. K_3C_{60}) have attracted much attention, and rather high transition temperatures above 30 K could be realized. More recently, interesting phenomena were observed in other alkali metal-doped organic molecular crystals such as the observation of an insulator–metal–insulator transition in alkali-doped phthalocyanines [5]. However, until recently superconductivity with high transition temperatures similar to those of the fullerides could not be observed in other molecular crystals despite many research activities, but recently superconductivity has been reported for another alkali metal-doped molecular solid, K_3 picene, with transition temperatures up to 18 K [6].

Here, we present the first comprehensive investigation of the electronic properties of undoped solid picene using state-of-the-art experimental tools and first-principles many-body calculations. Our results provide a detailed analysis of the occupied and empty states, confirming unambiguously the presence of four flat quasi-degenerate conduction bands that could give rise to a high density of states (DOS) around the Fermi level in the n-doped compound. Moreover, the measured spectral properties can only be accounted for if the anisotropy of the structure, local-field corrections and electronic correlations are taken into account.

The picene molecule is made of five benzene rings, as depicted in figure 1. In the condensed phase, picene adopts a monoclinic crystal structure, with lattice constants $a = 8.48 \text{ \AA}$, $b = 6.154 \text{ \AA}$, $c = 13.515 \text{ \AA}$ and $\beta = 90.46^\circ$, the space group is $P2_1$, and the unit cell contains two inequivalent molecules [7]. The molecules arrange in a herringbone manner, which is typical for many aromatic molecular solids.

2. Methods

For our photoemission studies, picene films with a thickness of about 6 nm were prepared by *in situ* thermal evaporation at an evaporation rate of 0.1 nm min^{-1} on a clean, polycrystalline gold substrate under ultra-high vacuum conditions. X-ray photoemission spectroscopy (XPS) and ultraviolet photoemission spectroscopy (UPS) experiments were carried out using a commercial PHI 5600 spectrometer equipped with two light sources. A monochromatized Al K_α source provided photons with an energy of 1486.6 eV for XPS. Photons with an energy of 21.21 eV (He discharge lamp) were used for valence band measurements. All UPS measurements were made by applying a sample bias of -5 V to obtain the correct, secondary electron cutoff that is required for determining the work function and the ionization potential. The recorded spectra were corrected for the contributions of He satellite radiation. The total energy resolution was about 350 meV (XPS) and 100 meV (UPS), respectively. The binding energy (BE) scale was aligned by measuring the Fermi edge (0 eV) and the $Au4f_{7/2}$ emission feature (84.0 eV) of the polycrystalline gold substrate. For further details of cleaning the substrate and characterization of films see the literature [8].

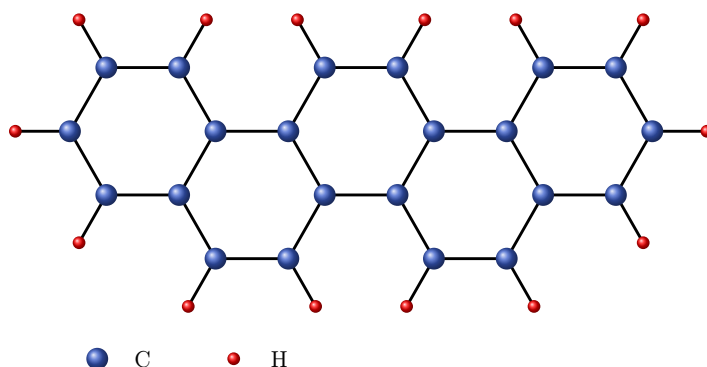


Figure 1. Schematic representation of the molecular structure of picene.

For our investigations using electron energy-loss spectroscopy (EELS) in transmission, we prepared picene films with a thickness of about 100 nm by thermal evaporation under high vacuum on single crystalline KBr substrates kept at room temperature. Two deposition rates, 0.2 and 4 nm min⁻¹, were chosen to obtain films with different crystal orientations. Subsequently, the picene films were floated off in distilled water and mounted on standard electron microscopy grids. Prior to the EELS measurements the films were characterized *in situ* using electron diffraction. All the observed diffraction peaks were consistent with the crystal structure of picene as given above. Moreover, the diffraction spectra revealed a pronounced texture: films grown with a deposition rate of 0.2 nm min⁻¹ showed a strong preference for crystallites having their *a*, *b*-plane parallel to the film surface, whereas films grown with 4 nm min⁻¹ showed a considerable number of crystallites having their *c*-axis on the film surface (see supplementary figure 6, available from stacks.iop.org/NJP/12/103036/mmedia). (For further details and additional figures see the supplementary data, available from stacks.iop.org/NJP/12/103036/mmedia.) The EELS measurements were carried out at room temperature using a 170 keV spectrometer that is described elsewhere [9]. We note that at this high primary energy, only singlet excitations are possible. We measured the loss function $\text{Im}(-1/\epsilon(\mathbf{q}, \omega))$ (where $\epsilon(\mathbf{q}, \omega)$ is the dielectric function) for a small momentum transfer \mathbf{q} as well as the core excitation from the C1s core level into unoccupied states. The energy and momentum resolution were chosen to be 85 meV and 0.03 Å⁻¹, respectively. The measured loss functions have been corrected for contributions from the elastic line [9]. For further details of the sample preparation procedure for EELS and the experimental technique, see [9, 10].

Experimental measurements were complemented by first-principles electronic structure calculations. Since density functional theory (DFT) in local density approximation (LDA) is known to underestimate band gaps [11], quasiparticle energies were calculated using the accurate *GW* self-energy approximation [12] of many-body perturbation theory, where the self-energy is given by the product of the Green's function *G* and the dynamically screened Coulomb interaction *W*. The crystal structure was optimized in LDA starting from experimental positions from [7]. We simulated the experimental loss functions in random-phase approximation (RPA) [11], using norm-conserving pseudopotentials (with an energy cutoff of 40 Ha in the plane-wave basis set), including 700 LDA bands in a 4 × 4 × 2 Monkhorst–Pack grid of \mathbf{k} points. Crystal local-field effects [11] are taken into account by inverting a matrix ϵ^{-1} of rank 73 \mathbf{G} vectors in the reciprocal space. For self-energy calculations, we have used 7000 plane waves in the expansion of the wavefunctions, 350 empty bands, a 6 × 6 × 4 Monkhorst–Pack \mathbf{k} -point

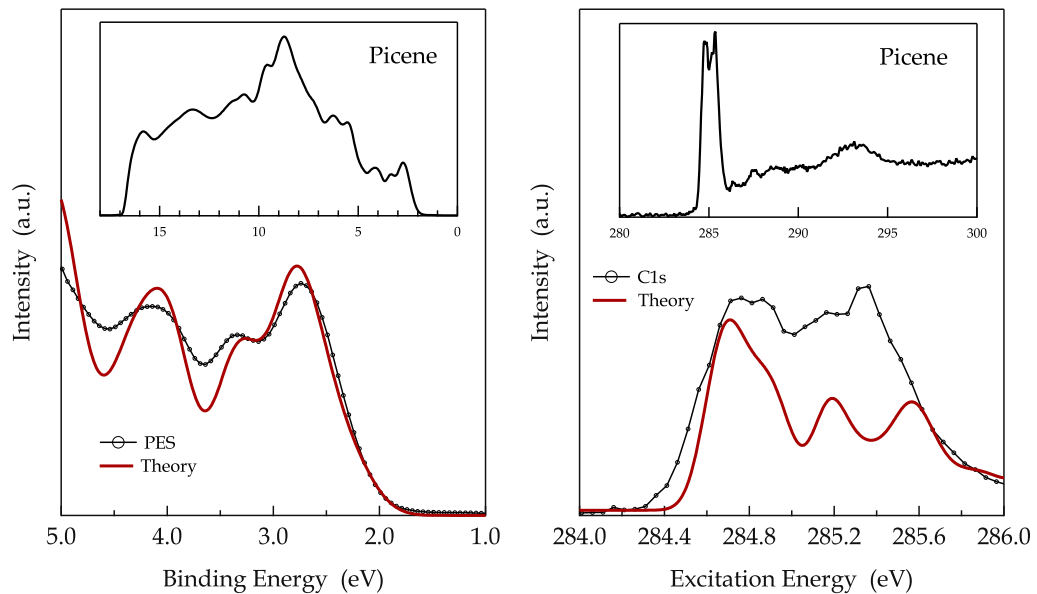


Figure 2. Left panel: valence band photoemission data of solid picene near the chemical potential. The inset shows the full spectrum including the secondary electron cutoff. Right panel: C1s excitation data of solid picene measured using EELS. The inset shows a much larger energy range. In the case of the C1s comparison, the theoretical data have been shifted such that the first peaks coincide.

grid and a plasmon-pole model approximation in the calculation of W . Quasiparticle energies are obtained as first-order corrections to LDA eigenvalues. For comparison, the calculated spectra have been convoluted with a Gaussian function of half-width 0.2 eV for the PES and 0.075 eV for the EELS.

3. Results and discussion

In the left panel of figure 2, we show the photoemission profiles of picene, which we compare with theoretical DOS, calculated within the accurate GW approximation of many-body perturbation theory. The structures closest to the chemical potential (BE = 0 eV) arise from the π -derived highest occupied molecular orbital (HOMO) of picene followed by deeper-lying electronic states (HOMO-1, HOMO-2, etc). Upon solid formation, these orbitals form bands with a relatively small bandwidth of about 0.5 eV (see supplementary figure 1) since the interaction between the molecules in solid picene is essentially van der Waals. Our calculations based on DFT using LDA follow the results of [13], but there is a major modification of the shape of the DOS if many-body correlation effects embedded in the GW approximation are taken into account. Quasiparticle corrections change the positions and intensities of the main peaks (see the detailed comparison in supplementary figure 2). The final result is in excellent agreement with the measured PES data. Below about 6–7 eV BE, we find that the σ -derived states additionally contribute to the photoemission spectrum. The spectral sharpness of the photoemission structures confirms that upon solid formation the molecular electronic states of picene remain relatively unchanged. Closest to the chemical potential, the photoemission data

reveal three maxima in the electronic DOS at 2.7, 3.35 and 4.15 eV, corresponding to the highest eight valence bands (see supplementary figure 1).

This observation demonstrates that the first occupied electronic levels of Picene are quite close in energy. The onset of the occupied electronic DOS is at about 2 eV below the chemical potential (or Fermi energy), which indicates quite a large band gap of solid picene. The ionization potential of solid picene determined using the data in figure 2 is 6.4 eV, i.e. picene is rather stable against oxidation. The work function of picene is thus 4.4 eV.

In the right-hand panel of figure 2, the C1s core excitation spectra of picene are depicted. Due to dipole selection rules, these data represent transitions into empty C2p-derived levels. In other words, core level EELS is able to probe the projected unoccupied electronic DOS of carbon-based materials [4, 14]. We thus compare the experimental EELS with the unoccupied DOS calculated in the GW approximation. Analogous to other π electronic systems, the features below 291 eV are caused by excitations into π^* -derived electronic states. The step-like structure at about 291 eV corresponds to the onset of transitions into σ^* -derived unoccupied levels. The C1s core excitation spectrum of picene shows a very sharp and dominating excitation feature right after the excitation onset at 284.3 eV, due to excitonic interactions with the core hole [14]–[16]. This excitation feature is characterized by a fine structure with maxima at 284.75, 284.85, 285.15 and 285.35 eV. These peaks are in very good agreement with the theoretical data if GW corrections are taken into account. From this analysis, we can unambiguously assign those structures to several unoccupied levels that are very close in energy (in the first 0.6 eV we count four bands and eight in the first 1.5 eV—see supplementary figure 1). Compared to pentacene (also made of five benzene rings, joined in a zigzag manner, instead of in an armchair-like manner as in picene), these bands show an even smaller dispersion [17]. When doped with electrons, these states become occupied, and this quasi-degeneracy has been proposed to cause a high DOS at the Fermi level in superconducting K_3 picene, a situation that resembles that in fullerenes and would be favourable for a relatively high transition temperature into the superconducting state. Moreover, this quasi-degeneracy of the conduction bands is also helpful in reducing the impact of electron correlation effects, i.e. to realize a metallic ground state similar to K_3C_{60} [1], which is a necessary prerequisite for superconductivity.

Finally, we present in figure 3 the loss function of solid picene, which provides insight into the electronic excitations of this compound. The experimental data presented in figure 3 are taken with a small momentum transfer \mathbf{q} of 0.1 \AA^{-1} , which represents the so-called optical limit [9]. Taking into account the anisotropic molecular and crystal structure of picene, it is reasonable to expect an anisotropic loss function as well. The theoretical results for the loss function, calculated in RPA, match the experimental measurements very well and provide fundamental insights with which to interpret the spectra.

For a momentum transfer \mathbf{q} parallel to the z -axis the loss function of picene is dominated by a broad structure at about 23 eV, which is attributed to the volume plasmon, a collective excitation of all valence electrons ($\pi + \sigma$ plasmon) (see supplementary figure 5). The well-structured loss function below 10 eV with clear maxima at about 4.6, 5.8, 6.4 and 7.3 eV in the experimental spectra is a signature of the energetically sharp and well-defined molecular electronic levels of picene, which remain relatively unchanged going to the solid state. The fact that the observed maxima with high intensity are close in energy is also in good agreement with the well-structured data shown in figure 2 for the electronic DOS, and we ascribe the excitation maxima in figure 3 to excitations between the energetically close-lying first occupied and unoccupied electronic states of picene. With respect to the experimental spectra, the theoretical

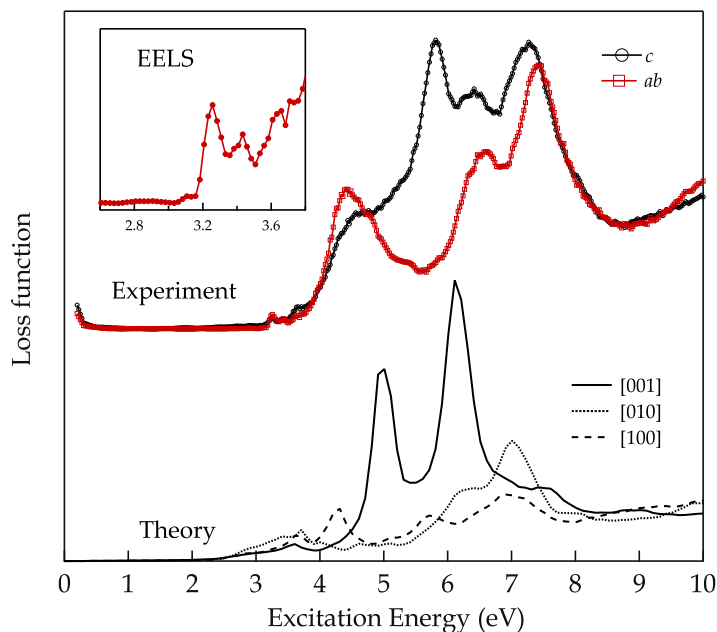


Figure 3. Loss function of solid picene at a small momentum transfer of 0.1 \AA^{-1} . The inset shows the spectrum close to the excitation onset. The experimental data represent excitations with predominant a , b polarization (labelled ab , red curves) and with a strong contribution of excitations polarized along the c -axis (labelled c , black curve).

results show a slight underestimation of the peak positions due to the fact that the band gap opening due to GW corrections and excitonic effects—both absent in the present calculations—do not compensate exactly for each other. From the analysis of the theoretical spectra we find that in the spectrum with \mathbf{q} parallel to the z -axis the first main structure at about 5 eV is located in the continuum of single-particle excitations and is due to interband transitions (seen as peaks in the imaginary part of ϵ , see supplementary figure 3). Instead, the second peak at about 6.1 eV occurs in correspondence to a zero of the real part of ϵ , where also the imaginary part is small. Therefore, this structure can be assigned to a plasmon, related to collective excitations with π character.

Comparing the EELS spectra with momentum transfer along the three directions, we note that moving from the z -axis towards the x -axis, the π and $\pi + \sigma$ plasmons undergo a blue shift and a red shift, respectively. This can be understood in terms of the one-particle excitations that originate them, as in layered systems like graphite and graphene [18, 19]. In fact, for \mathbf{q} directed along the z -axis (which is nearly parallel to the molecular main axis) $\pi - \sigma^*$ and $\sigma - \pi^*$ transitions have very small oscillator strength. Therefore, the main contributions in the low-energy and high-energy regions of the spectra are given by $\pi - \pi^*$ and $\sigma - \sigma^*$ transitions, respectively. On the other hand, when \mathbf{q} is directed along other directions, $\pi - \sigma^*$ and $\sigma - \pi^*$ transitions at intermediate frequencies increase their oscillator strength considerably. As a consequence, the main structures of the loss function in the low-energy (the π plasmon) and high-energy regions (the $\pi + \sigma$ plasmon) undergo a blue and a red shift, respectively. The anisotropic character of the loss function is also clearly visible when the effects of crystal local-fields (LFE) on the spectra are analysed. LFE are directly related to inhomogeneities in the induced charges (hence in the

induced Hartree potential). In fact, we find that LFE are almost negligible for \mathbf{q} parallel to the z -axis, i.e. along the main molecular axis, where the charge distribution is quite homogeneous, but LFE are stronger in the other directions as a manifestation of the inherent anisotropy of the molecular solid (see supplementary figure 4).

Zooming into the energy region around the excitation onset reveals an excitation onset in the experimental spectra, i.e. an optical gap, of 3.15 eV. This onset also represents a lower limit for the band gap (or transport energy gap) of solid picene. While the fundamental band gap is severely underestimated by the 2.39 eV LDA result (see also [13]), the GW band structure displays a direct quasiparticle gap of 4.08 eV (at the Z point of the Brillouin zone). The GW result also implies that in picene, one should expect an exciton BE larger than that in its close relative pentacene, where it is less than 0.5 eV [17], [20]–[22] and where a smaller band gap (2.3 eV) has also been reported [17, 22, 23]. The excitation onset of picene is followed by three rather weak electronic excitations at about 3.25, 3.4 and 3.65 eV. Following previous optical studies of picene molecules in solution [24], we attribute these low-lying (singlet) excitations to those that are polarized perpendicular to the long molecular axis, whereas at higher energies excitations polarized along this axis contribute. Again, there is a further clear difference from the electronic excitation spectrum of pentacene, where the electronic excitation across the energy gap has considerably greater relative spectral weight [25].

4. Summary

In conclusion, we have studied the electronic properties of picene using a combination of accurate experimental and theoretical spectroscopies. We analysed the results we obtained from photoemission spectroscopy and EELS to clarify the effects of electronic correlation and anisotropy on the dielectric response in order to understand its peculiar properties. With respect to pentacene, picene shows a larger quasiparticle gap, a larger exciton BE and a higher density of unoccupied states close to the Fermi energy.

Acknowledgments

We thank R Schönfelder, R Hübel and S Leger for technical assistance. We are grateful to the Deutsche Forschungsgemeinschaft for financial support (KN393/5 and KN393/9). This work was also supported by the Spanish MEC (FIS2007-65702-C02-01), ACI-Promociona (ACI2009-1036), ‘Grupos Consolidados UPV/EHU del Gobierno Vasco’ (IT-319-07), ETORTEK and by the European Union through e-I3 ETSF (contract 211956) and THEMAs (contract 228539) projects. We acknowledge support from the Barcelona Supercomputing Center (‘Red Espanola de Supercomputacion’). We have used Quantum Espresso [26], Abinit [27] and Yambo [28].

References

- [1] Gunnarsson O 2004 *Alkali Doped Fullerenes* (Singapore: World Scientific)
- [2] Weaver J H and Poirier D M 1994 *Solid State Physics* vol 48 (New York: Academic)
- [3] Forro L and Mihaly L 2001 *Rep. Prog. Phys.* **64** 649
- [4] Knupfer M 2001 *Surf. Sci. Rep.* **42** 1
- [5] Craciun M F *et al* 2006 *Adv. Mater.* **18** 320

- [6] Mitsuhashi R *et al* 2010 *Nature* **464** 76
- [7] De A *et al* 1985 *Acta Crystallogr. C* **41** 907
- [8] Peisert H *et al* 2003 *J. Appl. Phys.* **93** 9683
- [9] Fink J 1989 *Adv. Electron. Electron Phys.* **75** 121
- [10] Knupfer M *et al* 2000 *Chem. Phys. Lett.* **318** 585
- [11] Onida G *et al* 2002 *Rev. Mod. Phys.* **74** 601
- [12] Hedin L 1965 *Phys. Rev.* **139** A796
- [13] Kosugi T *et al* 2009 *J. Phys. Soc. Japan* **78** 113704
- [14] Knupfer M *et al* 1999 *Carbon* **37** 733
- [15] Shirley E L 1998 *Phys. Rev. Lett.* **80** 794
- [16] Soininen J A *et al* 2005 *Phys. Rev. B* **72** 045136
- [17] Tiago M L *et al* 2003 *Phys. Rev. B* **67** 115212
- [18] Marinopoulos A G *et al* 2002 *Phys. Rev. Lett.* **89** 076402
- [19] Marinopoulos A G *et al* 2004 *Phys. Rev. B* **69** 245419
- [20] Hill I G *et al* 2000 *Chem. Phys. Lett.* **327** 181
- [21] Zahn D R T *et al* 2006 *Chem. Phys.* **325** 99
- [22] Hummer K and Ambrosch-Draxl C 2005 *Phys. Rev. B* **71** 081202
- [23] Amy F *et al* 2005 *Org. Electron.* **6** 85
- [24] Gallivan J B and Brinen J S 1969 *J. Chem. Phys.* **50** 1590
- [25] Schuster R *et al* 2007 *Phys. Rev. Lett.* **98** 037402
- [26] Giannozzi P *et al* 2009 *J. Phys. Condens. Matter* **21** 395502
- [27] Gonze X *et al* 2005 *Z. Kristallogr.* **220** 558
- [28] Marini A *et al* 2009 *Comput. Phys. Commun.* **180** 1392